Practical estimation of veering effects on high-rise structures: a database-assisted design approach

DongHun Yeo*

National Institute of Standards and Technology, Gaithersburg, MD, USA
(Received December 29, 2010, Revised August 18, 2011, Accepted October 12, 2011)

Abstract. Atmospheric boundary layer winds experience two types of effects due to friction at the ground surface. One effect is the increase of the wind speeds with height above the surface. The second effect, called the Ekman layer effect, entails veering - the change of the wind speed direction as a function of height above the surface. In this study a practical procedure is developed within a database-assisted design (DAD) framework that accounts approximately for veering effects on tall building design. The procedure was applied in a case study of a 60-story reinforced concrete building, which also considered the dependence of veering effects on the orientation of the building. Comparisons are presented between response estimates that do not account for veering, and account for veering conservatively. For the case studied in this paper veering effects were found to be small.

Keywords: building technology; database-assisted design; mean recurrence interval; reinforced concrete; veering

1. Introduction

Atmospheric boundary layer winds experience two types of effects due to friction at the ground surface. One effect is the increase of the wind speeds with height above the surface. The second effect, called the Ekman layer effect, entails veering -- the change of the wind speed direction as a function of height above the surface. Much research has focused on effects of wind speed profiles, but veering effects on structures are far less documented in the archival literature.

Veering effects of interest for the design of high-rise structures include: (1) effects of continuous wind direction changes with height above ground, and (2) effects due to the difference between the directions of wind speed data at 10 m above terrain with open exposure on one hand and reference wind speeds at the roof level on the other. Neither type of effect can be studied in typical boundary layer wind tunnels, which do not have the capability to simulate veering.

In this study a practical procedure is developed within the database-assisted design (DAD) framework that approximately accounts for veering effects on tall building design. A case study is presented in which comparisons are made between structural responses with specified MRIs for buildings with various orientations, obtained (a) by not taking veering effects into account, and (b) by accounting for veering effects by using the approximate approach presented in this paper.

Veering in the atmospheric boundary layer is associated with the dependence on height of the

---

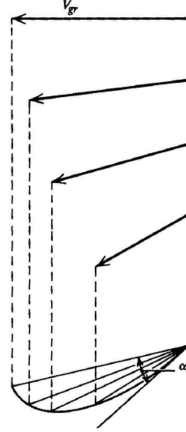* Corresponding author, Ph.D., E-mail: donghun.yeo@nist.gov

Fig. 1 Wind velocity directions in the atmospheric boundary layer, wind engineering convention (Simiu and Scanlan 1996)

balance of forces that govern air motion: the pressure gradient force, the Coriolis force, and the friction force, which vanishes at and above the gradient height, and increases from zero at the gradient height to its maximum value at the ground surface. Fig. 1 shows that the wind direction in the atmospheric boundary layer describes a spiral, called the *turbulent Ekman spiral*. The angle between the direction of the wind speed at the gradient height and at the surface is defined in meteorological terms as the veering angle. The veering angle is counterclockwise in the northern hemisphere and clockwise in the southern hemisphere. The veering angle has little variation within the region from elevation zero to elevation z_l where the logarithmic law holds. This follows from the assumption that, throughout this region, the shear stress differs little from the surface stress (Schlichting 1960, Simiu and Scanlan 1996), meaning that, below the elevation z_l, the velocity component normal to the shear stress and, therefore, the change in the veering angle, is small. Note that the gradient height is higher than the height z_l.

The height z_l is proportional to the shear velocity (i.e., it is a function of the wind speed at any specified reference height, say, at 10 m above ground), and is inversely proportional to the Coriolis parameter, Therefore z_l is greater in strong than in moderate winds and, for equally strong winds, it is smaller at higher than at lower latitudes. The dependence of z_l on speed has been documented by measurements in a rotating wind tunnel (Howroyd and Slawson 1975), in extratropical storms (Thuillier and Lappe 1964), and in hurricanes, for which z_l is of the order of a few hundred meters (Powell *et al.* 2003).

Fig. 2 shows approximate values of veering angles at 500 m elevation (10° for open terrain, and 15° for densely built suburban terrain) suggested by Powell (2005). Note that the suggested veering angles do not account for angle of latitude or wind speed. Because z_l is an increasing function of wind speed and a decreasing function of angle of latitude, the values of the suggested veering angles are likely to be conservative for strong winds and low latitudes.

These considerations suggest that the quantitative determination of veering angles is still imperfect and approximate. For this reason it is not yet possible to estimate veering effects "exactly" on the basis of existing measurements in atmospheric flow. Nor is it possible to estimate veering effects in either conventional boundary layer wind tunnels or large-scale aerodynamic facilities of the "Wall of Wind" type. Therefore, we believe that the development of a rational, approximate, and conservative

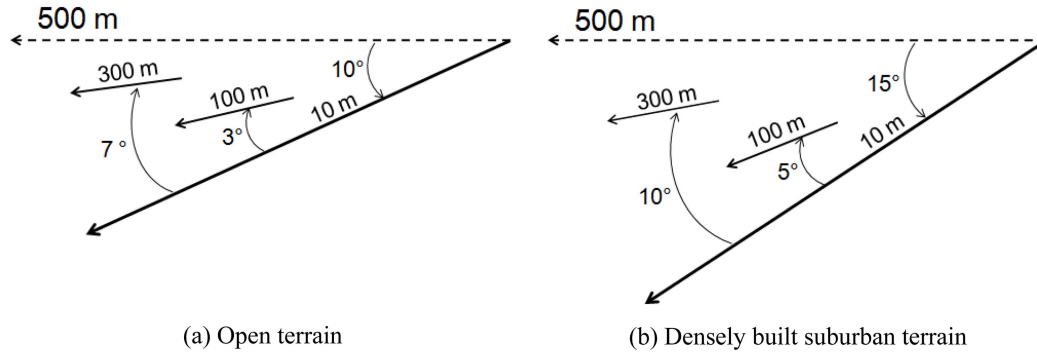(a) Open terrain   (b) Densely built suburban terrain

Fig. 2 Suggested values of veering angles (Powell 2005)

procedure for performing such estimates is warranted. Such a procedure is proposed herein. The procedure is based on the assumption that the order of magnitude of estimates of veering angles proposed by Powell (2005) is reasonably correct, and offers estimates of upper bounds of veering effects based on those estimates. The proposed procedure fills a gap in the archival literature on tall building design which, to our knowledge, does not offer structural engineers any guidance to the estimation of upper bounds of veering effects. Such upper bounds are developed in this paper by assuming that veering, rather than increasing gradually with height, is uniform over the entire height of the building. This is equivalent to changing the building orientation by an angle equal to the difference between the veering angle at the surface and the veering angle at the top of the building. This change can either increase or decrease the estimated wind effects. If the estimated wind effects are increased by the appropriate change in building orientation, it is the increased wind effect that is taken into account in the structural calculations. If the estimated wind effects are decreased, the decrease is not taken into account in structural design. This approach assures that veering effect is accounted for conservatively. Another factor that contributes to the conservatism of our estimates of veering effects is the strength of the across-wind loading on the structure. The variation of the direction of wind speeds with height tends to reduce the across-wind effects. The approach based on DAD techniques used in this paper, which automatically account for across-wind effects, disregards that reduction, hence the additional conservatism of this approach. However, the following caveat is in order. For conservative estimates to be assured, the angular resolution for the aerodynamic testing must be sufficiently high. In testing the structure in the wind tunnel it is therefore necessary to increase the angular resolution in situations where abrupt changes in the aerodynamics of the building may be expected for small variations in the wind direction.

As the case study presented in the paper shows, the conservatism inherent in our approach is relatively mild, at least for buildings comparable to the 300 m tall building investigated in the paper. This is, in our opinion, a useful result, which to our knowledge has so far not been reported in the archival literature. In the event that, for the building of interest, the conservatism inherent in our approach turns out to be relatively severe, the designer has the option of attempting a more accurate estimation of veering effects than our approach can provide. Such an estimation is in principle possible by using rotating wind tunnels that can simulate Coriolis effects (Howroyd and Slawson 1975, Simiu and Scanlan 1996).

2. Procedure for estimating veering effects on building response

In wind engineering practice, as well as in this paper, the veering angle, denoted by α, rather than being defined as in the preceding paragraphs, is defined as the difference between the wind direction at the surface of the Earth and the direction at the height of interest. The veering angle so defined is clockwise in the Northern hemisphere and counterclockwise in the Southern hemisphere. As represented in Fig. 2, the veering angles at 100 m and 300 m above ground are then about 3° and 7° over open terrain, respectively, and 5° and 10°, respectively, over densely built suburbs (Powell 2005); for suburban terrain with roughness intermediate between open and densely built suburban terrain the values of the veering angles may be assumed to be about 4° at 100 m and about 8° - 9° at 300 m. These values, which are tentative, were assumed in the case study presented in this work. Note that according to Dyrbye and Hansen (1997), however, the veering angle at higher elevations (i.e., about 1 km) is 20°, and according to Holmes (2007) it is 30°.

By convention we consider the North direction as the origin of the angular coordinate β defining wind direction at 10 m above the surface. For example, for wind blowing from the East at 10 m above the surface, $\beta = 90°$. Owing to veering, in the Northern hemisphere wind blowing from direction β at 10 m above the surface will have the direction $\beta + \alpha$ at higher elevations. (In the Southern hemisphere the direction at higher elevations will be $\beta - \alpha$.) For convenience we consider henceforth only wind in the Northern hemisphere.

The orientation of the building is defined by the angle θ_{or} between the North direction and a principal axis of the building denoted by x (Fig. 3). The angle between the direction of wind blowing from direction β at 10 m above the surface and a principal axis is then $\beta - \theta_{or}$. Owing to veering, at a higher elevation the angle between that wind and the principal axis x is $\beta - \theta_{or} + \alpha$. For example, let the angle θ_{or} be 30°. Consider a 300 m tall building with open exposure. For an eastern wind (wind blowing from direction $\beta = 90°$ at 10 m above the surface) the angle between that direction and the principal axis x is $90° - 30° = 60°$ at 10 m above the surface. Owing to veering the direction of the eastern wind changes at higher elevations. At the top of the building the direction of the wind blowing from the East at 10 m above the Earth's surface will be 97° with
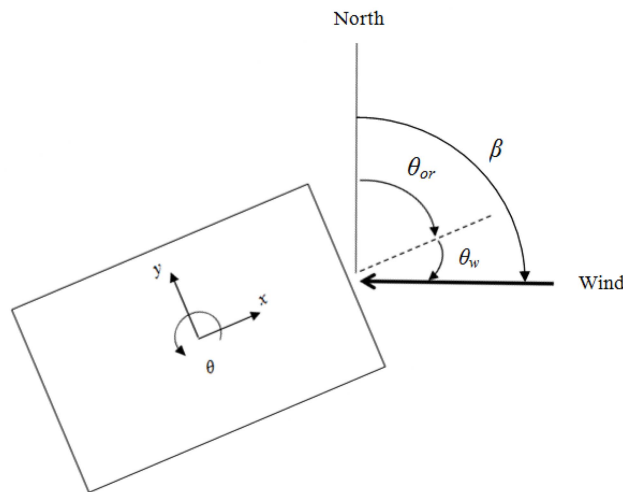

Fig. 3 Angles defining building orientation and wind direction at 10 m above the Earth's surface

respect to the North direction, and the angle θ_w between that direction and the x axis of the building will be $97^\text{o} - 30^\text{o} = 67^\text{o}$.

The effects of veering are estimated in this study by calculating the response in two ways. First, the response of the structure subjected to wind loads is calculated by disregarding veering. Second, the response is calculated by taking veering into account. Because wind tunnels typically do not simulate veering, it is necessary in calculations to resort to a simplified model of veering. In this model the veering angle is constant over the entire building height and is equal to the assumed veering angle at the top of the building. This model typically results in conservative estimates of veering effects on the building response.

In this work veering effects are studied within the framework of the database-assisted design (DAD) technique, which requires the following wind engineering input: (1) an aerodynamic database of the pressure coefficient time histories at a sufficiently large number of taps on the building model envelope, (2) a local climatological database of wind speeds at the standard elevation (typically 10 m above ground over open terrain), and (3) a micro-meteorological data set consisting of ratios between mean hourly wind speeds at the elevation of the building rooftop and the corresponding directional 3-s or 10-min wind speed at the standard elevation of the meteorological site. Once the wind engineering input is available, the response calculations can be performed by using the High-Rise Database-Assisted Design for Reinforced Concrete Structures (HR_DAD_RC) software. The procedure on which the software is based is now described. For details see Yeo (2010).

1. A time series of pressure coefficients are used to produce the time series of (a) horizontal wind force components along the principal axes of the building, applied at the center of mass of each floor or group of floors, and (b) torsional moments about those centers of mass. This task is performed separately for each wind direction, and for wind speeds blowing from that direction of, say, 20 m/s, 30 m/s,…, 80 m/s. The outputs of this task are time series of wind loads induced by winds with those speeds, for every wind direction being considered (e.g., 0°, 10°,…, 350°, or 0°, 22.5^o,…, 337.5^o). Note that this task is independent of the wind climate at or near the building site, and that the output just mentioned is an aerodynamic property of the building.

2. A dynamic analysis of the building is performed for each wind speed and direction listed in item 1 above. This analysis yields the respective time histories of the inertial forces and torsional moments acting at and around the centers of mass of the floors or groups of floors being considered. The sums of the applied wind loads and of the inertial loads represent the total wind-induced loads acting on the structure.

3. Once the total horizontal wind loads are available, HR_DAD produces time series of the wind effects of concern by multiplying the total loads by the appropriate influence coefficients. The wind effects being calculated should be those that are of direct concern to the designer. The member design is checked using (a) interaction equations of internal forces due to wind effects and gravity loads and (b) the section capacity. (These are referred to as demand-to-capacity indexes (DCIs), and typically consist of demand-to-capacity ratios.) Additional wind effects of concern are inter-story drift and top floor accelerations. Note that all the wind effects are calculated for each of the wind directions and for each of the wind speeds listed in item 1 above. This task is performed automatically by the HR_DAD software. Its output consists of *wind effect databases* (also referred to as *response databases*) representing the wind effects being sought as a function of wind direction and wind speed. This output is also a property of the structure, independent of wind climate at or near the site. In a response database the wind directions are referenced with respect to a principal
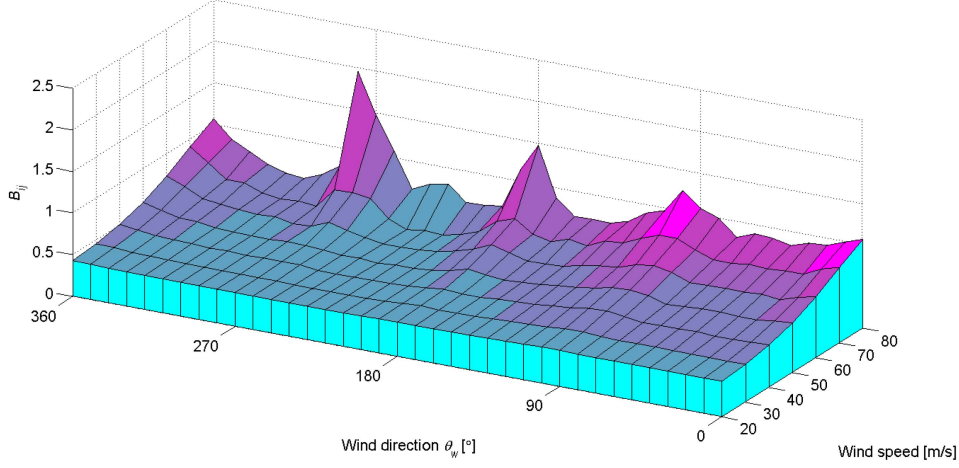
Fig. 4 Example of a wind effects database. The wind effects consist for this plot of a set of demand-to-capacity index B_{ij} for a tall building column

axis of the building. For an example see Fig. 4.

4. The wind effect databases enable the conversion of the $m \times n$ matrix, whose elements are directional wind speeds v_{ij} (m is the number of windstorm events or years of record and n is the number of wind directions; $i = 1, 2, ..., m$; $j = 1, 2, ..., n$), into a matrix with the same dimensions whose elements are wind effects (e.g., individual member DCIs, inter-story drift, and top floor accelerations) induced by the directional wind speeds v_{ij}. Denote the elements of this matrix by r_{ij}. For each row of the matrix whose elements are r_{ij}, only the wind effect $\max_j (r_{ij})$ is of interest from a structural design viewpoint and is therefore retained. The requisite operations are performed automatically by the HR_DAD software, giving rise to the vector $\max_j (r_{ij})$. That vector is rank-ordered, and given the arrival rate of the wind storm events, each of its m rank-ordered components corresponds to an MRI automatically calculated by the HR_DAD software.

Veering effects are taken into account in item 4 above. Two wind effects are estimated assuming: (1) no veering, and (2) approximate veering. For the no veering case, the response database is rotated clockwise by the angle of building orientation θ_{or}; owing to this rotation, the wind directions considered in the response database are referenced with respect to the same angular origin (i.e., the North direction) as the wind directions at 10 m above ground, rather than with respect to the principal axis x of the building. For the approximate veering case, the response database is rotated clockwise by the angle $\theta_{or} + \alpha$. The wind effects of interest based on assumptions (1) and (2) above are used for veering effects estimation. Note that for the response database and the wind climatological database used in the HR_DAD calculations the reference height of all winds is the top of the building, just as it is for the aerodynamic database obtained in the wind tunnel. Note that the estimation of veering effects is dependent on resolution of the directional wind datasets being used, which in this study is 22.5°. A wind climatological database with a higher resolution will estimate the veering effects more accurately.

3. Structural response

The loads induce in the structure three types of response of interest in design: demand-to capacity indexes (Sect. 3.1), inter-story drift (Sect. 3.2), and accelerations at the top floor (Sect. 3.3). For details see Yeo (2010).

3.1 Demand-to-capacity indexes

The demand-to-capacity index (DCI) is a quantity used to measure the adequacy of a structural member from the point of view of strength. In general, this index is defined as a sum of ratios of internal forces induced by the design loads at a member cross section to the strength available at that cross section. The design strength in HR_DAD_RC is based on the Building Code Requirements for Structural Concrete and Commentary 318-08 (hereinafter ACI 318-08). An index higher than unity indicates that the design of a structural member is inadequate. The HR_DAD_RC software employs two DCIs: one for axial or/and flexural loads, and one for shear and torsion.

The index "B_{ij}^{PM}" pertains to the axial load and bending moment for columns, and to and bending moments for beams. Depending upon whether the section is controlled by tension or compression, the index has the form

$$B_{ij}^{PM} = \frac{M_u}{\phi_m M_n} \quad \text{(for a tension-controlled section)}$$
$$= \frac{P_u}{\phi_p P_n} \quad \text{(for a compression-controlled section)} \tag{1}$$

where M_u and P_u are the bending moment and axial force at the section being considered, M_n and P_n are the nominal moment and axial strengths at that section, and ϕ_m and ϕ_p are the capacity reduction factors for flexural and axial strengths, respectively. In particular, for columns subject to bi-axial flexure loads, the Bresler reciprocal load method of R10.3.6 in ACI 318-08 (2008) is used for compression-controlled sections, and the PCA (Portland Cement Association) load contour method (PCA 2008) is used for tension-controlled sections; these methods involve sums of terms similar to those of Eq. (1).

The index "B_{ij}^{VT}" is associated with interaction equation for shear forces and torsional moment for columns and beams

$$B_{ij}^{VT} = \frac{\sqrt{V_u^2 + \left(\frac{T_u p_h b_w d}{1.7 A_{oh}^2}\right)^2}}{\phi_v (V_c + V_s)} \tag{2}$$

where V_c and V_s are the nominal shear strengths provided by the concrete and the reinforcement, respectively, V_u is the shear force, T_u is the torsional moment, ϕ_v is the reduction factor for shear strength, p_h is the perimeter enclosed by the centerline of the outermost closed stirrups, A_{oh} is the area enclosed by the centerline of the outermost closed stirrups, b_w is the width of the member, and d is the distance from the extreme compression fiber to the centroid of longitudinal tension reinforcement.

3.2 Inter-story drift

The time series of inter-story drifts at the ith story, $d_{i,x}(t)$ and $d_{i,y}(t)$ (Fig. 5) corresponding to the x and y axes, respectively, are

$$d_{i,x}(t) = \frac{[x_i(t) - D_{i,y}\theta_i(t)] - [x_{i-1}(t) - D_{i-1,y}\theta_{i-1}(t)]}{h_i}$$

$$d_{i,y}(t) = \frac{[y_i(t) - D_{i,x}\theta_i(t)] - [y_{i-1}(t) - D_{i-1,x}\theta_{i-1}(t)]}{h_i} \tag{3}$$

where $x_i(t)$, $y_i(t)$, and $\theta_i(t)$ are the displacements of and the rotation about the mass center at the ith floor, $D_{i,x}$ and $D_{i,y}$ are distances along the x and y axes from the mass center on the ith floor to the point of interest on that floor, and h_i is the ith story height (i.e., the vertical distance between the mass centers of the ith and the $(i-1)^{th}$ floor).

The ASCE 7-05 Commentary (2005) suggests limits on the order of 1/600 to 1/400 for an annual probability of exceedance of 0.05, i.e., for a mean recurrence interval (MRI) of 20 years (see Section CC.1.2 in ASCE 7-05).

3.3 Top floor acceleration

The time series of the resultant acceleration at the top floor, $a_r(t)$ is obtained in HR_DAD_RC by the expression

$$\alpha_r(t) = \sqrt{[\ddot{x}_{top}(t) - D_{top,y}\ddot{\theta}_{top}(t)]^2 + [\ddot{y}_{top}(t) - D_{top,y}\ddot{\theta}_{top}(t)]^2} \tag{4}$$

where the accelerations $\ddot{x}_{top}(t)$, $\ddot{y}_{top}(t)$, and $\ddot{\theta}_{top}(t)$ of the mass center at the top floor pertain to the x, y, and θ (i.e., rotational) axes, and $D_{top,x}$ and $D_{top,y}$ are the distances along the x and y axes from the mass center to the point of interest on the top floor.

The resultant value in Eq. (4) is used, instead of accelerations along the principal axes, because the peak acceleration is of concern regardless of its direction. ASCE 7-05 does not provide wind-related peak acceleration limits. However, for office buildings, a limit of 25 mg for a 10-year MRI was suggested by Isyumov *et al*. (1992) and Kareem *et al*. (1999).
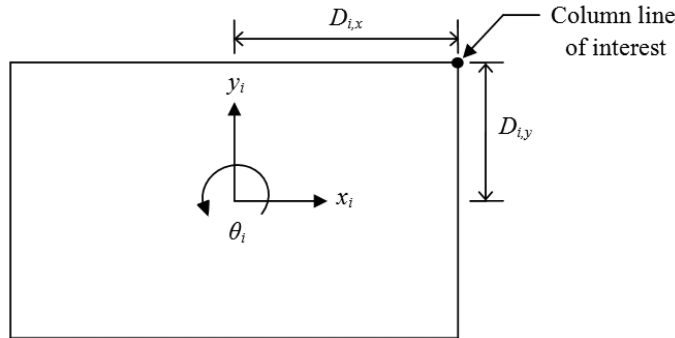

Fig. 5 Position parameters at floor i for inter-story drift

4. Case study and results

A 60-story reinforced concrete building with rigid diaphragm floors was designed using the software High-Rise Database-Assisted Design for Reinforced Concrete structures (HR_DAD_RC) developed by NIST (Yeo 2010). The building, known as the Commonwealth Advisory Aeronautical Research Council (CAARC) building, has dimensions 45.72 m in width, 30.48 m in depth, and 182.88 m in height. It has a moment-resistant frame structural system consisting of 2880 columns and 4920 beams, and is similar to the structural system studied by Teshigawara (2001). The building was assumed to be located near Miami, Florida and have suburban exposure. For details see (Yeo 2010).

Time histories of aerodynamic wind loads on each floor were calculated from time series of pressure coefficients on a rigid wind tunnel model of the CAARC building. The aerodynamic data were obtained at the Inter-University Research Center on Building Aerodynamics and Wind Engineering (CRIACIV-DIC) Boundary Layer Wind Tunnel in Prato, Italy (Venanzi 2005). The loads for 36 wind directions (10° increments) were obtained from directional pressure data measured from taps on the envelope of the building. Fig. 6 shows a typical set of four structural members selected for the calculation of wind effects. For estimates of DCIs structural members were chosen as follows: a corner column (*cc*), a non-corner column (*cn*), an exterior beam (*be*), and an interior beam (*bi*). Mean recurrence intervals (MRIs) of 300 years, 700 years, and 1700 years were considered. The indexes for MRI = 300 years are not appropriate in a 60 story building; however, they were employed in this study for comparisons with results obtained for higher MRIs.

The climatological database used in the study is a wind speed dataset of 999 simulated hurricanes for 16 directions near Miami (Milepost 1450), obtained from the site www.nist.gov/wind (Batts *et al*. 1980). The angles indicating those directions (β) are from 22.5° to 360° clockwise from the
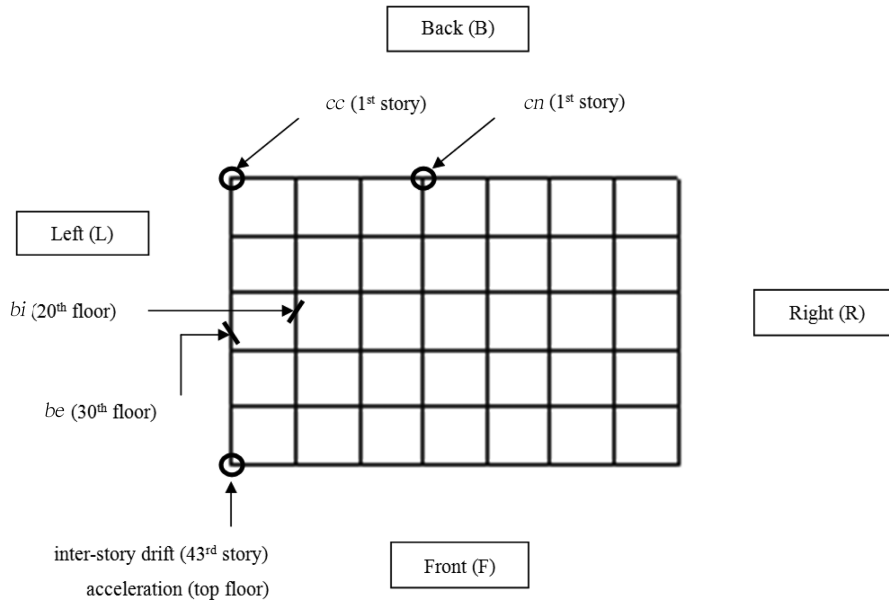

Fig. 6 Plan view of building with locations of selected members (θ_{or} = 90°) (*cc* = corner column; *cn* = internal column; *be* = exterior beam; *bi* = interior beam)

(for no veering, B_{ij}^{PM} ⋯⋯ , B_{ij}^{VT} ⋯⋯ ; for approximate veering, B_{ij}^{PM} —— , B_{ij}^{VT} ----)
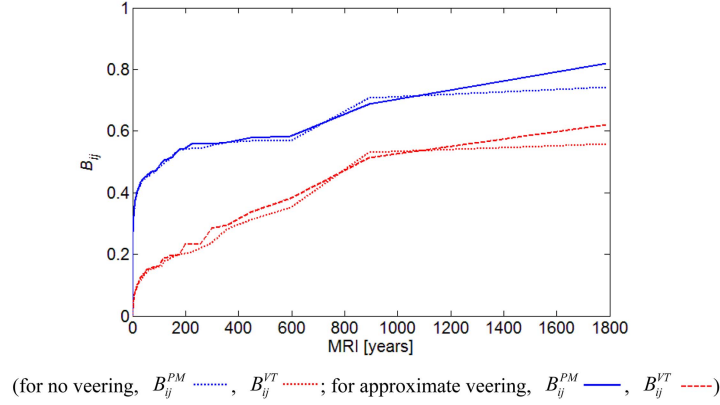
Fig. 7 Demand-to-capacity indexes as functions of MRIs for building orientation ($\theta_{or} = 90^{\circ}$)

North in 22.5° increments. Other hurricane wind speeds data sets are available commercially.

Because the wind climatological database corresponds to open exposure in all directions, the veering angle is estimated to be 5° from 10 m to the building roof elevation (i.e., 182.88 m) by linear interpolation from Fig. 2. For each of the 999 storm events only the largest of the 16 directional responses is of interest and is retained. This yields a vector of the 999 largest directional responses. The peak response database, consisting of the vector of those 999 values, allows the estimation of the peak response corresponding to specified MRIs through the use of the non-parametric estimation method described in of Simiu and Miyata (2006), Sect. 2.4.3.2.2. Note that the MRIs pertain to load effects, not to wind loads.

Fig. 7 shows peak response databases for demand-to-capacity indexes of the corner column (*cc*) for the building orientation $\theta_{or} = 90^{\circ}$. Differences between indexes corresponding to the no veering case and to the approximate veering case are negligible for low MRIs, and remain modest for high MRIs.

Fig. 8 compares DCIs for the no-veering case and for the approximate veering case. For a given building orientation, the larger of the DCIs for these two cases is considered in design. Fig. 9 shows DCIs based on (a) estimates of veering effects and (b) no veering effects, for 300-year and 1700-year MRI, respectively.

It is seen that veering effects on DCIs are stronger for higher MRIs, and are larger for columns than for beams. This is due to the strong directional dependence of the responses for high wind speeds. For the index B_{ij}^{PM} of the corner column the veering effects are very small for MRI = 300 years but increase by up to approximately 20% for MRI = 1700 years. As the MRI increases, the veering effects become larger, in particular for certain building orientations. The B_{ij}^{PM} indexes for the 1700-year MRI vary as functions of building orientation from 0.73 to 0.93 for the corner column, 0.74 to 0.84 for the non-corner column, 0.50 to 0.66 for the exterior beam, and 0.55 to 0.73 for the interior beam. For B_{ij}^{VT} the DCIs for MRI = 1700 years increase by approximately 30% and 10% owing to the veering effects for columns and beams, respectively. Their dependence on building orientation is also observed.

Note that for very tall buildings, for which veering effects may be of interest, the design is typically governed by serviceability constraints, and internal forces in structural members are typically smaller than those members' capacity. This is the case for the building investigated in this
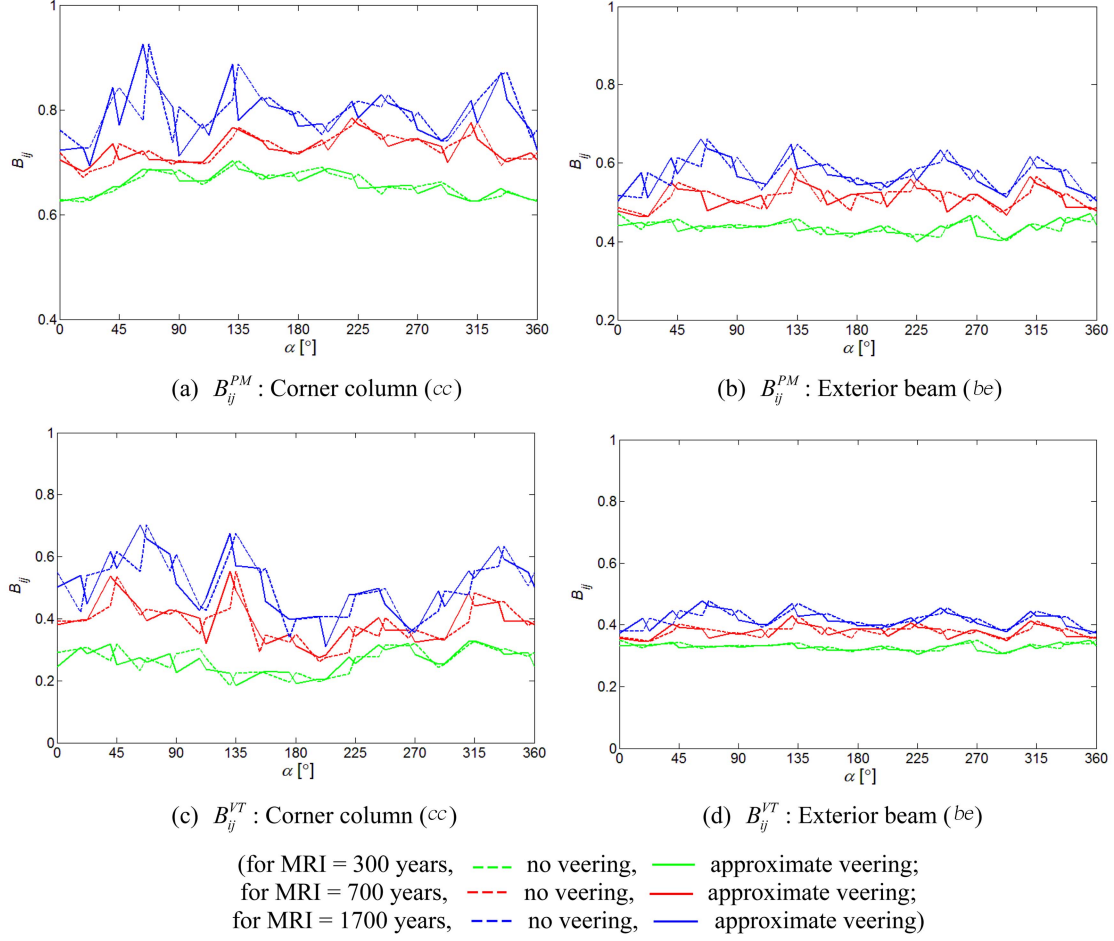
(a) B_{ij}^{PM} : Corner column (cc)   (b) B_{ij}^{PM} : Exterior beam (be)

(c) B_{ij}^{VT} : Corner column (cc)   (d) B_{ij}^{VT} : Exterior beam (be)

(for MRI = 300 years,   --- no veering,   —— approximate veering;
for MRI = 700 years,   --- no veering,   —— approximate veering;
for MRI = 1700 years,   --- no veering,   —— approximate veering)

Fig. 8 Peak demand-to-capacity indexes

(for B_{ij}^{PM} with veering effects,   —— MRI = 300 years,   —— MRI = 1700 years;

for B_{ij}^{PM} without veering effects,   ·········· MRI = 300 years,   ·········· MRI = 1700 years;

for B_{ij}^{VT} with veering effects,   —— MRI = 300 years,   —— MRI =1700 years;

for B_{ij}^{VT} without veering effects,   ·········· MRI = 300 years,   ·········· MRI =1700 years)
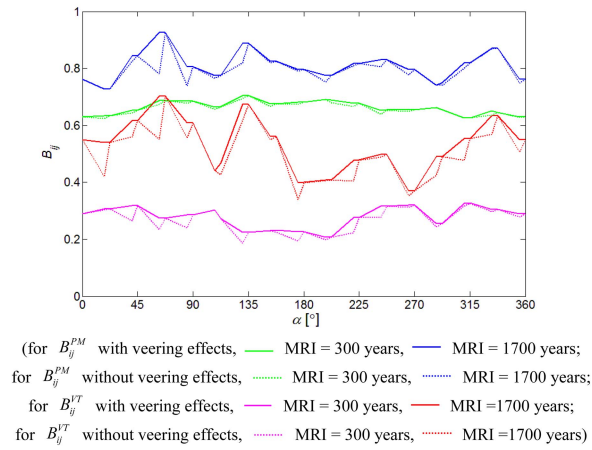
Fig. 9. Demand-to-capacity indexes of corner column (cc) with or without veering effects

section, for which the demand-to-capacity indexes B_{ij}^{PM} and B_{ij}^{VT} are seen to be less than unity even if the conservatively estimated veering effect is taken into account.

Inter-story drift was calculated for a 20-year MRI, along the principal axes (i.e., x and y) and as a resultant of the x and y components, for the front-left corner of the 43rd story (Fig. 6). Veering effects were found to be about 3% or less. The variation of veering effects with building orientation was also found to be small (less than 10%).

Peak top floor acceleration for a 10-year MRI was estimated for the front-left corner along the x-axis defining building orientation (Fig. 6). Acceleration increases due to veering do not exceed 5%, and do not exhibit significant directionality preference due to building orientation.

The results show that serviceability design can ignore veering effects because these responses have low sensitivity to wind direction at MRIs of the order of, say, 20 years.

5. Conclusions

Procedures for the estimation of veering effects of interest in the design of high-rise structures have not been presented in the archival literature because typical boundary layer wind tunnel measurements cannot account for the continuous change of wind direction with height above the surface. Rather than seeking an "exact" estimation of veering effects, this study presents a practical and conservative procedure for estimating upper bounds of veering effects. The procedure uses database-assisted design (DAD) techniques and estimates (1) wind effects unaffected by veering, and (2) wind effects affected by veering assumed to be uniform over the building height, rather than varying gradually from the surface to the top of the building. The wind effects considered in design are the larger of these two estimated wind effects and are therefore estimated conservatively. In addition, the proposed procedure automatically accounts for across-wind effects, and does so again conservatively, insofar as it disregards the weakening of vortex shedding effects due to the change in wind direction over the building height. However, the following caveat is in order. For conservative estimates to be assured, the angular resolution for the aerodynamic testing must be sufficiently high. In testing the structure in the wind tunnel it is therefore necessary to increase the angular resolution in situations where abrupt changes in the aerodynamics of the building may be expected for small variations in the wind direction.

For the case studied in this paper veering effects were found to be relatively small. The conservatism inherent in our approach is relatively mild, at least for buildings comparable to the 300 m tall building investigated in the paper. This is, in our opinion, a useful result, which to our knowledge has so far not been reported in the archival literature. The conclusions based on this application would clearly differ for different types of building or conditions. In the event that, for the building of interest, the conservatism inherent in our approach turns out to be relatively severe, the designer has the option of attempting a more accurate estimation of veering effects by resorting, e.g., to rotating wind tunnels that are capable of simulating Coriolis effects.

Software for implementing the DAD procedure used in this study is available on www.nist.gov/wind. To the author' knowledge this is the first study that quantifies effects of veering on high-rise buildings by using a documented estimation method available in the public domain.

Acknowledgements

The author would like to thank Dr. Emil Simiu of the National Institute of Standards and Technology for his advice and comments. The wind tunnel data used in this paper were obtained at the Inter-University Research Centre on Building Aerodynamics and Wind Engineering (CRIACIV-DIC) Boundary Layer Wind Tunnel, Prato, Italy provided by Dr. Ilaria Venanzi of the University of Perugia.

References

ACI (2008), *Building code requirements for structural concrete (ACI 318-08) and commentary*, American Concrete Institute, Farmington Hills, MI.

ASCE (2005), *Minimum design loads for buildings and other structures*, American Society of Civil Engineers, Reston, VA.

Batts, M.E., Russell, L.R. and Simiu, E. (1980), "Hurricane wind speeds in the United States", *J. Struct. Division-ASCE*, **106**(10), 2001-2016.

Dyrbye, C. and Hansen, S.O. (1997), *Wind loads on structures*, John Wiley & Sons.

Holmes, J.D. (2007), *Wind loading of structures*, Spon Press, New York.

Howroyd, G.C. and Slawson, P.R. (1975), "The characteristics of a laboratory produced turbulent Ekman layer", *Bound-Lay Meteorol.*, **8**(2), 201-219.

Isyumov, N., Fediw, A.A., Colaco, J. and Banavalkar, P.V. (1992), "Performance of a tall building under wind action", *J. Wind Eng. Ind. Aerod.*, **42**(1)-(3), 1053-1064.

Kareem, A., Kijewski, T. and Tamura, Y. (1999), "Mitigation of motions of tall buildings with specific examples of recent applications", *Wind Struct.*, **2**(3), 201-251.

PCA (2008), *PCA notes on 318-08 building code requirements for structural concrete with design applications*, Portland Cement Association, Skokie, IL.

Powell, M.D. (2005), personal communication.

Powell, M.D., Vickery, P.J. and Reinhold, T.A. (2003), "Reduced drag coefficient for high wind speeds in tropical cyclones", *Nature*, **422**(6929), 279-283.

Schlichting, H. (1960), *Boundary layer theory*, McGraw-Hill, New York.

Simiu, E. and Miyata, T. (2006), *Design of buildings and bridges for wind: a practical guide for ASCE-7 Standard users and designers of special structures*, John Wiley & Sons, Hoboken, NJ.

Simiu, E. and Scanlan, R.H. (1996), *Wind effects on structures*, John Wiley & Sons.

Teshigawara, M. (2001), *Structural design principles (chapter 6)*, Imperial College Press, London.

Thuillier, R.H. and Lappe, U.O. (1964), "Wind and temperature profile characteristics from observations on a 1400 ft tower", *J. Appl. Meteorol.*, **3**(3), 299-306.

Venanzi, I. (2005), *Analysis of the torsional response of wind-excited high-rise building*, Ph.D. Dissertation, Università degli Studi di Perugia, Perugia.

Yeo, D. (2010), *Database-assisted design of high-rise reinforced concrete structures for wind: Concepts, software, and application*, NIST Technical Note 1665, National Institute of Standards and Technology, Gaithersburg, MD.

CC